HEAVY ION PHYSICS WITH CMS*

David J. Hofman

On behalf of the CMS Collaboration

University of Illinois at Chicago, Chicago, IL 60607, USA

(Received November 15, 2006)

The study of heavy ion collisions at the Large Hadron Collider (LHC) represents an opportunity to study partonic matter at center-of-mass energies a factor of ~ 27 times higher than currently possible. This dramatic increase in energy will allow the creation of strongly interacting matter at the highest energy density ever produced in the laboratory. The Compact Muon Solenoid (CMS) detector is ideally suited to study the rich physics of Quantum Chromodynamics and the strong interaction in this new energy region. A brief overview of the heavy ion physics capabilities of the CMS detector is presented.

PACS numbers: 25.75.–q

1. Introduction

Our current understanding of how bulk partonic matter behaves with increasing energy density is based on results from heavy ion collisions up to a maximum energy of $\sqrt{s_{NN}} = 200\,\mathrm{GeV}$, currently achievable at the Relativistic Heavy Ion Collider (RHIC). There is compelling evidence that the hot QCD matter created in this 200 GeV energy region behaves as a strongly interacting collective medium that also has a significant effect on fast partons traversing it [1]. Global particle production from this hot medium was also found to exhibit many simple scaling relationships, which provide a baseline for extrapolation to the LHC energy region of $\sqrt{s_{NN}} = 5.5\,\mathrm{TeV}$ and an immediate data-driven starting point for potential new discoveries [2]. The LHC expands the heavy ion physics possibilities in kinematics (Q^2 and x) and new probes. For example, the dramatic energy increase at the LHC enhances cross sections, often by orders of magnitude, for the production of high p_{T} jets, photons, heavy quark particles and Z^0 bosons, many of which

* Presented at the "Physics at LHC" Conference, Kraków, Poland, July 3–8, 2006.

are not even experimentally accessible at RHIC. The CMS detector has the capability to make measurements that take advantage of these exciting physics opportunities.

2. Overview of the CMS detector

A research program in high energy heavy ion physics has been part of the CMS Collaboration's plans since inception. Although the CMS detector was designed and optimized to maximize the physics potential from high-luminosity p–p running, this same design is also optimal in many ways for running with heavy ions at the expected full luminosity of $5 \times 10^{26}\,\mathrm{cm}^{-2}\mathrm{s}^{-1}$ for Pb+Pb collisions. Below we briefly outline the CMS detector and its performance for fully simulated heavy ion collisions.

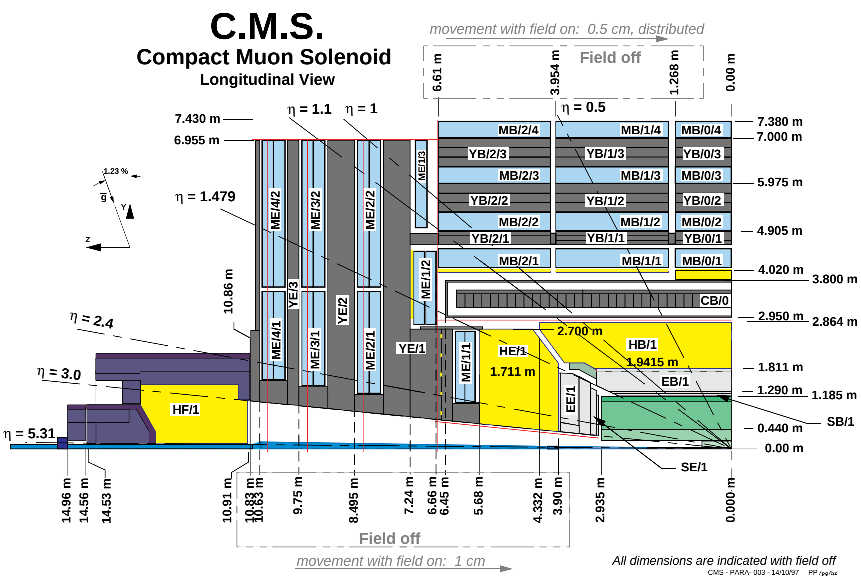

Fig. 1. A vertical slice through one quadrant of the CMS detector. The other three quadrants are identical and symmetric about the center of the interaction region and about the beam axis.

The CMS detector was designed to provide both high resolution tracking and superior granularity calorimetry with coverage over a full 2π azimuthal angle out to high pseudorapidity. The layout and dimensions of one quadrant of the CMS primary detector components are shown in Fig. 1. Starting from the nominal interaction point, for $|\eta| < 2.4$ particles will first traverse the silicon tracker (not labeled), then the electromagnetic ("EB" and "EE") and hadronic ("HB" and "HE") calorimeters and finally the trackers ("MB" and

"ME") for muons. The magnet coil is labeled as CB, and absorbers for the muon detectors are integrated into the magnet return yoke ("YB" and "YE"). Additional calorimetry in the forward region ("HF") provides complete calorimetry coverage out to $|\eta| < 5$.

Fig. 2 shows the CMS detector coverage in the η–ϕ plane for the muon trackers, calorimeters (HCAL and ECAL) and silicon trackeås well as the additional coverage provided by more forward calorimeters, CASTOR ($5.3 < |\eta| < 6.7$) [3] and the ZDC ($|\eta| > 8$ for neutrals) [4], which are not shown in Fig. 1.

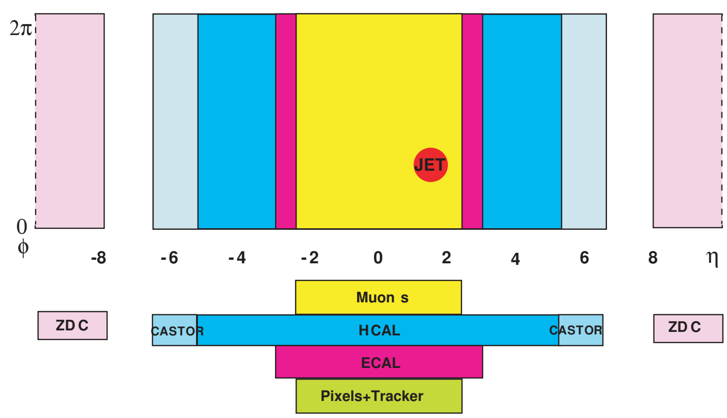

Fig. 2. Acceptance of tracking, calorimetry, and muon identification in pseudorapidity and azimuth. For illustration, the size of a jet with cone $R = 0.5$ is shown.

2.1. Silicon detector tracking in CMS

The CMS silicon tracker [5] is a 1.1 m radius cylindrical detector, 5.5 m long, immersed in the 4 T solenoid magnetic field. The Si tracker itself consists of a barrel component, covering $|\eta| < 2.1$, and end-cap disks that extend coverage to $|\eta| < 2.5$. The barrel component contains three highly-segmented ($100 \times 150\,\mu\text{m}^2$) pixel layers surrounded by four inner strip counters ($80\,\mu\text{m} \times 6.1\,\text{cm}$) and six outer strip counters ($\sim 150\,\mu\text{m} \times 9.1\,\text{cm}$). The pixel layers are located close to the interaction point, at radii of 4.4, 7.5 and 10.2 cm from the beam. The end-cap contains two pixel layers surrounded by three inner strip and nine outer strip detectors. Selected layers are instrumented with a double-sided configuration, and all together the Si tracker provides up to 17 independent measurements per track in the barrel, and 21 in the end-cap. Another important feature of the CMS Si tracker is that in addition to the digital hit positions, the pulse height information from each sensor will be recorded.

The performance of the Si tracker in the heavy ion environment was evaluated using fully simulated central Pb+Pb collisions for a wide range of maximum midrapidity charged particle yields, $dN_{\rm ch}/dy|_{y=0}$. A value of $dN_{\rm ch}/dy|_{y=0} \approx 3000$, as illustrated in the left panel of Fig. 3, corresponds to a charged particle density close to the maximum expected from extrapolation of lower energy data. The right panel of Fig. 3 gives the resulting occupancy in the Si barrel detector. The high segmentation of the Si pixel wafers results in a channel occupancy of 1–2% for measurements closest to the collision point and less than 10% for the outermost Si strip layers.

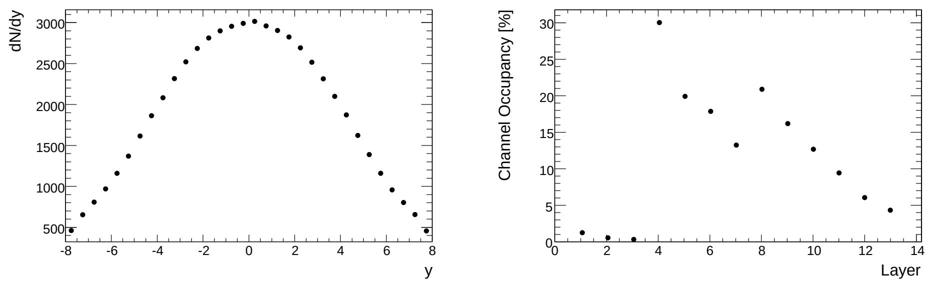

Fig. 3. (Left) Simulated charged particle density in central Pb+Pb collisions as a function of rapidity. (Right) Channel occupancy in the barrel region as a function of detector layer for the particle yields shown in the left-hand-side. Layer 1–3 correspond to the pixel detector, 4–7 to the inner and 8–13 to the outer Si-strip tracker.

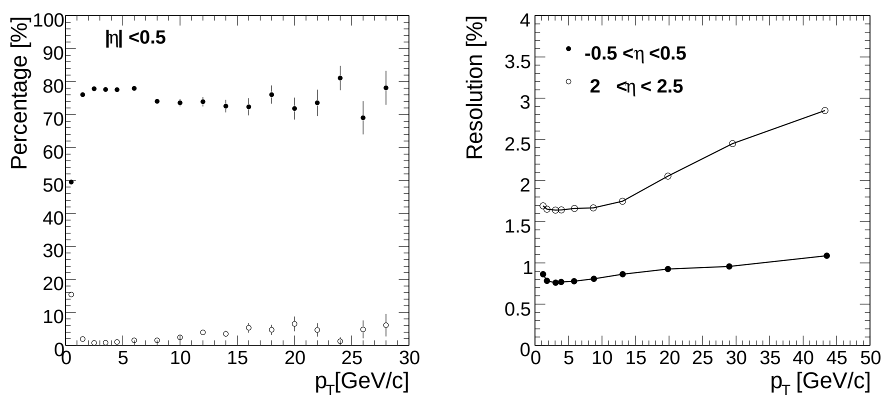

Fig. 4. (Left) Track reconstruction efficiency (full symbols) and fake track rate (open symbols) as a function of transverse momentum near midrapidity for central Pb+Pb collisions with $dN_{\rm ch}/dy|_{y=0} \approx 3000$. Track quality cuts in this figure are optimized for a low fake track rate (see text). (Right) Transverse momentum ($p_{\rm T}$) dependence of the track resolution achieved in heavy ion events in the Si barrel region (full symbols) and in the forward region (open symbols).

The charged particle track reconstruction performance for central Pb+Pb collisions is shown in Fig. 4. An algorithmic efficiency of $\sim 75\%$ is achievable when optimizing for low fake rates $< 5\%$ [6]. Efficiencies of $\sim 88\%$ with fakes $\sim$10% are possible when optimizing for high efficiency. The high granularity of the Si tracker, in combination with the 4 T magnetic field, gives an excellent momentum resolution of $\Delta p_{\mathrm{T}}/p_{\mathrm{T}} < 1.5\%$ in the Si barrel region and <3% in the Si end-cap region up to high transverse momenta.

2.2. Calorimetry in CMS

One of the strengths of the CMS detector is the extensive coverage with both electromagnetic [7] and hadronic [8] calorimetry. The central electromagnetic calorimeter, with coverage $|\eta| < 3$, consists of 75848 scintillating $PbWO_4$ crystals arranged in both barrel and end-cap sections (see Fig. 1). The crystal face dimensions of 22 mm^2 correspond to an excellent granularity of $\Delta\eta \times \Delta\phi \sim 0.0175 \times 0.0175$ in the barrel region, and their length of 230 mm provides 25.8 X_0 (radiation lengths). The hadronic barrel and end-cap calorimeter consist of alternating scintillators and copper plates that correspond to 5.15 λ_{I} (interaction lengths) in the barrel region. The forward calorimeter ($3 < |\eta| < 5$) is a steel plus quartz–fiber Cherenkov design that consists of both electromagnetic and hadronic sections.

In addition to the extensive pseudorapidity coverage outlined above, CMS has the best coverage of forward angles among the LHC experiments thanks to the CASTOR and zero-degree (ZDC) calorimeters (see Fig. 2). CASTOR [3] is an azimuthally symmetric electromagnetic and hadronic Čerenkov-light calorimeter that consists of successive layers of tungsten absorber and quartz plates arranged to provide $\sim 22\,X_0$ and $10.3\,\lambda_{\mathrm{I}}$. The ZDC [4] is also a tungsten and quartz sampling Čerenkov calorimeter with electromagnetic and hadronic sections providing $19\,X_0$ and $5.6\,\lambda_{\mathrm{I}}$, respectively.

The possibility, for the first time, to measure identified jets in heavy ion collisions represents an exciting new physics opportunity at the LHC. Measurements of fully-formed jets will be possible through utilization of the extensive calorimetry coverage of CMS outlined above. The jet reconstruction performance of the CMS calorimetry in a heavy ion environment is made difficult by the necessity to identify localized E_{T} clusters on top of the substantial background from the underlying event. Despite the challenges, the CMS heavy ion analysis is made possible by utilizing an event-by-event η-dependent background subtraction scheme coupled with an iterative jet cone-finder algorithm [9]. This fast method of jet reconstruction using only the calorimeter information is available at the trigger level, and already provides excellent reconstruction efficiency and purity, as shown in the left panel of Fig. 5. The energy resolution, shown as a function of E_{T} in the right panel of Fig. 5, is $\approx 16\%$ for 100 GeV jets, and the jet location resolutions in η and ϕ are 0.028 and 0.032, respectively.

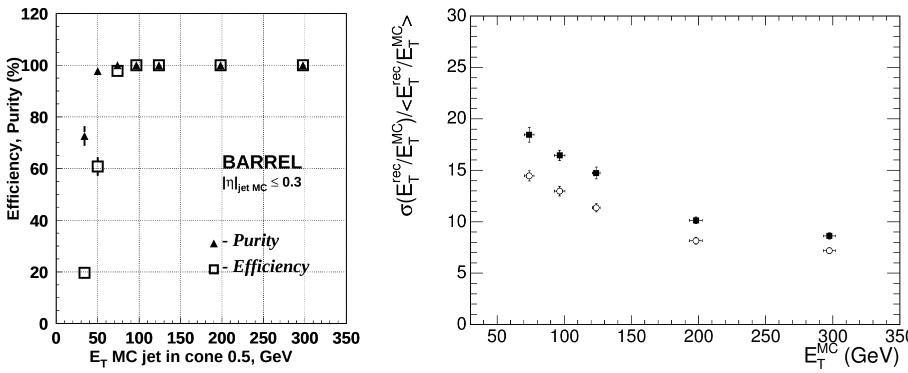

Fig. 5. (left) Jet reconstruction efficiency and purity using the barrel calorimeters for PYTHIA generated jets embedded in a Pb+Pb heavy ion background with $dN_{\mathrm{ch}}/dy|_{y=0} \approx 5000$, which is above the maximum expected at $\sqrt{s_{NN}}$=5.5 TeV. (Right) Jet transverse energy resolution determined for the same Pb+Pb heavy ion collisions (closed symbols) compared to proton+proton (open symbols).

2.3. Muon reconstruction in CMS

As implied by its name, the CMS detector is ideal for muon reconstruction with excellent coverage of $|\eta| < 2.5$ over the complete 2π in azimuth [10]. Muons are tagged by the muon chambers inserted into the return yoke of the CMS magnet, as shown in Fig. 1, and additional resistive plate chambers designed for trigger purposes cover $|\eta| < 2.1$. The barrel tracking is provided by drift tubes with 2.5 m long anode wires, arranged in four groups (or stations) of 12 planes each. This design allows each station to provide an independent 3-dimensional point on the muon trajectory. Cathode strip chambers are utilized in the end-cap, where each of the 24 layers measure both the radial and azimuthal position of the trajectory.

The performance of the muon reconstruction in a heavy ion environment is excellent. This is primarily due to the ability to cleanly tag muon tracks and match them to the corresponding track measured in the CMS Si tracker in order to calculate the momentum with high resolution. As an example, this procedure applied to Pb+Pb events with $dN_{\mathrm{ch}}/dy|_{y=0} \approx 3000$ results in a reconstructed mass resolution for $\Upsilon \to \mu^+\mu^-$ of 90 MeV/c^2 for the full range $|\eta| < 2.4$ and 53 MeV/c^2 in the midrapidity region ($|\eta| < 0.8$) [11].

2.4. Data acquisition and triggering in CMS

The demands on the CMS Trigger and DAQ system are substantial. Full luminosity $p + p$ running at the LHC will result in a 40 MHz (beam crossing) interaction rate. To deal with this challenge, CMS has designed a two level trigger system [12], as illustrated in Fig. 6. The first level, Level-1, is implemented with custom electronics and reduces the $p+p$ event rate down to 100 kHz. All subsequent online selection is performed by the High Level Trigger (HLT), which consists of a large scalable cluster of commercial workstations. The effective output to permanent storage from the HLT is limited to ~ 225 MByte/sec, or ~ 150 Hz in $p + p$ collisions.

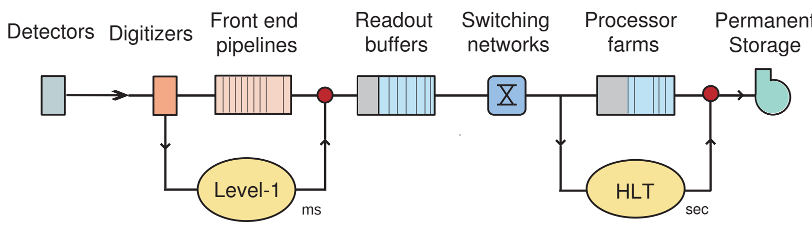

Fig. 6. Schematic of the data flow through the CMS Trigger and DAQ.

In heavy ion collisions the situation is somewhat different. The peak collision rate for Pb+Pb is only ~ 8 kHz, which means that every event can be sent to the HLT for detailed inspection. Therefore, the main purpose of the Level-1 trigger in heavy ion running will be to provide a clean discrimination of true collisions from all possible background sources and perhaps to provide seed objects such as high p_{T} muon candidates as input to the HLT. The HLT software environment allows complex algorithms to be run on fully built events, and provides great flexibility to create specialized heavy ion trigger algorithms without the necessity of hardware reconfiguration.

3. Heavy ion physics potential of CMS

As discussed briefly above, the CMS detector design has excellent performance for heavy ion collisions and the physics potential is correspondingly very high. The CMS Collaboration will perform heavy ion physics studies that span a wide range of phenomena, including soft physics and global properties of the produced medium, the production and propagation of high p_{T} particles and jets, quarkonia yields, as well as forward physics and low-x QCD measurements.

The large acceptance of CMS, together with the excellent calorimetry in the very forward region, will allow detailed studies of triggering, event selection and centrality determination biases. These effects must be understood before moving on to global observables of great interest that include measurements of particle production, collective phenomena such as elliptic flow, as well as particle spectra and correlations.

The extensive calorimetry available for jet reconstruction will allow comprehensive studies of high p_{T} probes such as detailed measurements of jet fragmentation including its centrality and flavor dependence as well as azimuthal asymmetry. The CMS muon capabilities will allow precision measurements of the properties and yields of quarkonia [11]. The combination of Si tracking, calorimetry and muon detection provides for additional studies including jet $+\gamma$ and jet $+Z^0$ correlations. The far forward detectors will provide CMS with coverage for essential measurements of parton distribution functions in both protons and nuclei as well as shed light on the nature of the predicted low-x gluon saturation [13].

Active work continues on detailed simulations of a wide range of heavy ion physics measurements in CMS, including those listed above.

REFERENCES

[1] BRAHMS, PHOBOS, STAR and PHENIX Collaborations on physics from RHIC, *Nucl. Phys.* **A757**, 1 (2005).

[2] B.B. Back *et al.* PHOBOS Collaboration, *Nucl. Phys.* **A757**, 28 (2005).

[3] A.L.S. Angelis, A.D. Panagiotou, *J. Phys. G* **23**, 18 (1997); P. Katsas *et al.*, submitted to *Nucl. Instrum. Methods* **A**.

[4] O.A. Grachov *et al.*, Proceedings of the CALOR 2006, `nucl-ex/0608052`; C. Adler *et al., Nucl. Instrum. Methods* **A470**, 488 (2001).

[5] The CMS Collaboration, CERN/LHCC 98-6; CERN/LHCC 2000-016.

[6] C. Roland *et al.*, CMS-NOTE/2006-031 (2006).

[7] The CMS Collaboration, CERN/LHCC 97-33.

[8] The CMS Collaboration, CERN/LHCC 97-31.

[9] The CMS Collaboration, CERN/LHCC 2006-001.

[10] The CMS Collaboration, CERN/LHCC 97-32.

[11] M. Bedjidian, O. Kodolova, CMS-NOTE/2006-089.

[12] The CMS Collaboration, CERN/LHCC 2000-38.

[13] D. d'Enterria, Proceedings of the Hot-Quarks'06, `hep-ex/0609019`.